

Original Article

Diffusional kurtosis imaging in evaluating the secondary change of corticospinal tract after unilateral cerebral infarction

Shun Zhang¹, Wenjie Zhu¹, Yan Zhang¹, Yihao Yao¹, Jingjing Shi¹, Cong-Yi Wang², Wenzhen Zhu¹

¹Department of Radiology, Tongji Hospital, Tongji Medical College, Huazhong University of Science and Technology, Wuhan, China; ²The Center for Biomedical Research, Key Laboratory of Organ Transplantation, Ministry of Health & Ministry of Education, Tongji Hospital, Tongji Medical College, Huazhong University of Science and Technology, Wuhan, China

Received December 17, 2016; Accepted February 7, 2017; Epub March 15, 2017; Published March 30, 2017

Abstract: We investigated to evaluate whether diffusional kurtosis imaging (DKI) can early detect the microstructure change of corticospinal tract (CST) after unilateral cerebral infarction solely in middle cerebral artery (MCA) territory. Seventy-seven patients with MCA territory infarct consisting of 10 subjects of hyperacute phase, 22 subjects of acute phase, 28 subjects of subacute phase and 17 subjects of chronic phase were enrolled in this study. ROI method was performed to measure the mean value of the infarcted area and the areas which belongs to CST [including the posterior limb of internal capsule (PLIC), cerebral peduncle (CP), pons, and medulla] in both ipsilateral and contralateral mirror side in all the DKI-derived parametric maps. Compared with the contralateral mirror side, MK, K_{\parallel} , K_{\perp} in the infarcted area sharply increased to a peak in acute phase, and then gradually fell down. MD, D_{\parallel} and D_{\perp} decreased till acute phase and then started to increase gradually. FA decreased more and more seriously from hyperacute to chronic phase. K_{\parallel} and D_{\parallel} were more helpful to detect the subtle changes of CST after infarction as they both had significant changes in all phases. Moreover, there were more locations that had significant changes with time going on. To conclude, DKI, especially the variable K_{\parallel} and D_{\parallel} , may serve as a new biomarker to observe the microstructure change of the descending CST, which may reflect the extent of Wallerian degeneration and be helpful for clinical decision making.

Keywords: Diffusional kurtosis imaging, corticospinal tract, Wallerian degeneration, middle cerebral artery occlusion

Introduction

Ischemic stroke often results in hemiparesis, aphasia, and sensory disturbances, which brings great social and family problems. After stroke, corticospinal tract (CST) Wallerian degeneration, which is associated with poor neurological outcome [1], is often seen subsequently in about 1~3 months or later in conventional MRI examinations. Wallerian degeneration is the secondary degeneration of distal axons after regional injury of the neuronal cells, which is commonly seen after stroke. In the early phase, the corticospinal tract in conventional T_1WI , T_2WI or FLAIR images often appears normal. Diffusion weighted imaging (DWI) [2, 3] and diffusion tensor imaging (DTI) [4-7], T_2 relaxation time [2] have been used to observe

the subtle change of CST. FA decreased significantly in ipsilateral corticospinal tract after ischemic stroke compared to the contralateral side, and FA value correlated well with motor function scale, while T_2 relaxation time failed to detect the Wallerian degeneration.

Diffusional kurtosis imaging (DKI) is a quantitative measure of the non-Gaussianity of the diffusion process in both white matter and gray matter; it has more advantages over DTI and can yield additional kurtosis information. Initial results proved that DKI may better characterize the complexity or heterogeneity of tissue microenvironment, and has more sensitivity [8-11]. Till now, little DKI related studies about the CST Wallerian degeneration have been systematically evaluated. The purpose of this study is to

Table 1. Detailed information about the recruited patients

	Hyperacute phase	Acute phase	Subacute phase	Chronic phase
Time from symptom onset to MRI examination	< 6 hours	> 6 hours ~3 days	> 3 days ~10 days	> 10 days ~30 days
No.	10	22	28	17
Sex (M/F)	8/2	17/5	18/10	13/4
Age (years)	55.80 ± 14.59	53.59 ± 12.28	55.71 ± 9.72	51.29 ± 10.67

characterize the ischemic lesion with DKI, and to evaluate whether DKI derived variables can early detect the microstructure change of CST after unilateral cerebral infarction solely in middle cerebral artery (MCA) territory.

Materials and methods

Patient selection

This study was approved by the ethics committee of local institution, and written informed consent was acquired from all subjects. Seventy-seven patients from 114 ischemic stroke patients were recruited in the study. All the included subjects satisfied the following criteria: (1) patients that experienced unilateral ischemic stroke in sole MCA territory which confirmed in DWI and conventional MR sequences; (2) the ischemic lesions did not involve the posterior limb of internal capsule (PLIC); (3) the patients had never suffered from stroke or other neurological diseases before.

The final 77 patients (56 male and 21 female) aged from 24 to 80 years, 54.14 ± 11.30 years) were classified as four phases according to the time from their symptom onset to MRI examination: (1) hyperacute phase (less than 6 hours, $n = 10$, 8 male and 2 female, 55.80 ± 14.59 years); (2) acute phase (> 6 hours ~3 days, $n = 22$, 17 male and 5 female, 53.59 ± 12.28 years); (3) subacute phase (> 3 days ~10 days, $n = 28$, 18 male and 10 female, 55.71 ± 9.72 years); (4) chronic phase (> 10 days ~30 days, $n = 17$, 13 male and 4 female, 51.29 ± 10.67 years). The patients' information is summarized in **Table 1**.

MRI examination

All the subjects were examined on GE Discovery MR750 3.0Tesla MR scanner (Gradient field switching rate is 200 T/ms) with a 32-channel head coil. The imaging sequences included T_1 WI, T_2 WI, FLAIR, DWI ($b = 1000$ s/mm²) and DKI. Imaging parameters for DKI were as follows: field of view (FOV) = 24 cm, slice thick-

ness/spacing = 4.0/0.0 mm, TR/TE = 5000/98.1 ms, matrix = 128 × 128, Bandwidth = 250.0, NEX = 1, $b = 0, 1250, 2500$ s/mm² (diffusion encoding vectors along 25 directions for every non-zero b value). The total scanning time was 5 minutes and 45 seconds.

Data post processing

All the DKI raw images were processed using the software (Diffusional Kurtosis Estimator, version 2.0, http://academicdepartments.musc.edu/cbi/dki/DKE/dke_download.htm) developed by Tabesh et al [12]. Before DKI calculation, we checked all the diffusion images to make sure that there was no significant image distortion. Then, the DKI raw images were processed step by step according to the Diffusional Kurtosis Estimator. Firstly, all the DICOM images were converted to NIFTI format using MRICron, and the images with $b = 1250$ and $b = 2500$ s/mm² were registered to $b = 0$ images using SPM8. Then a voxel-by-voxel analysis was made and both diffusion kurtosis and diffusion tensor were estimated simultaneously. These co-registered images were fitted with a nonlinear fitting algorithm (DKI fitting) with all the data ($b = 0, 1250, 2500$ s/mm²) were used. The following diffusion kurtosis and diffusion tensor parametric maps were generated as: mean kurtosis (MK), axial kurtosis (K_{\parallel}), radial kurtosis (K_{\perp}), fractional anisotropy (FA), mean diffusion coefficient (MD), axial diffusion coefficient (D_{\parallel}) and radial diffusion coefficient (D_{\perp}) maps. They were fitted to the following Equation:

$$\ln[S(n, b)/S_0] = -b \sum_{i=1}^3 \sum_{j=1}^3 n_i n_j D_{ij} + \frac{1}{6} b^2 \overline{D}^2 \sum_{i=1}^3 \sum_{j=1}^3 \sum_{k=1}^3 \sum_{l=1}^3 n_i n_j W_{ijkl}$$

where $S(n, b)$ is the signal intensity for non-zero b -value along direction n , S_0 is the signal intensity for $b = 0$ (without any diffusion gradient), n_i, n_j, n_k and n_l are the components of the direction vector D_{ij} and W_{ijkl} denote the components of the 2nd order diffusion tensor D and the 4th order kurtosis tensor K , respectively, and \overline{D} is the MD.

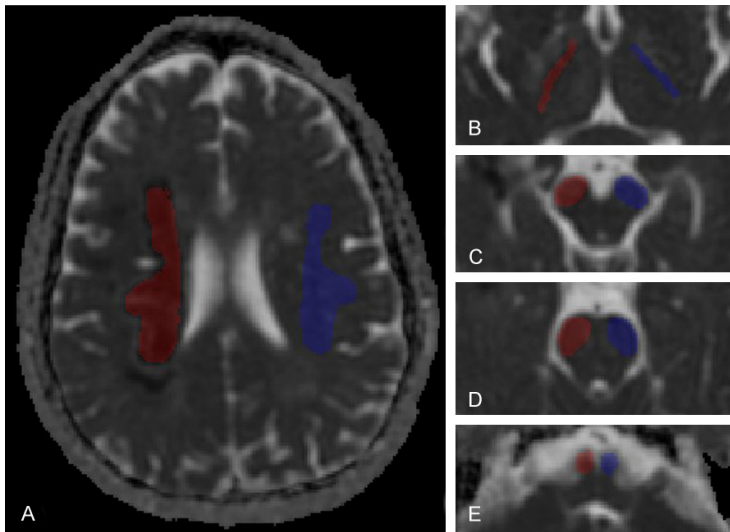


Figure 1. ROIs in the plane of lesion (A) and the four selected plane of corticospinal tract [PLIC (B), CP (C), pons (D), and medulla (E)] on MD map. Red color represents ROIs ipsilateral to the lesion, and blue color represents ROIs contralateral to the affected side.

Region of interests (ROIs) were manually drawn in transverse slices using ImageJ software (<http://rsb.info.nih.gov/ij/>) from MD map, and then projected to other parametric maps. The ROIs include the infarcted area (Lesion), ipsilateral posterior limb of internal capsule (ipsilateral PLIC), ipsilateral cerebral peduncle (ipsilateral CP), ipsilateral pons, ipsilateral medulla and the same area on the contralateral mirror side, including the contralateral Lesion (Mirror), contralateral PLIC, contralateral CP, contralateral pons and contralateral medulla. The ROIs in PLIC, CP, pons, and medulla were drawn along the corticospinal tract (CST) (**Figure 1**). All the ROIs were drawn by an experienced neuroradiologist (5 years) and checked by another neuroradiologist (8 years) simultaneously.

Statistics analysis

The statistical analysis was performed using SPSS software for Windows (version 19.0, Chicago, IL) and $P < 0.05$ was recognized as the significance criteria. Paired t test was used to compare the differences between the two sides in all the DKI-derived variables.

Results

Comparison of DKI-derived variables between infarcted area and the contralateral mirror area

MK, K_{\parallel} and K_{\perp} in the infarcted area demonstrated irregular high signal, while MD, D_{\parallel} , D_{\perp}

and ADC showed relatively homogeneous low signal. FA exhibited low signal with the boundary ambiguously (**Figure 2**).

Compared to the contralateral mirror area, MK, K_{\parallel} , K_{\perp} sharply increased with the time, and increased to the peak in acute phase (1.864 ± 0.475 , 1.650 ± 0.357 , 2.045 ± 0.540), then gradually decreased (**Figure 3**). MK, K_{\parallel} , K_{\perp} increased by 96.36%, 134.51%, 65.13% in the peak compared with the contralateral mirror side, respectively. Except for K_{\perp} in chronic phase ($P = 0.135$), MK, K_{\parallel} and K_{\perp} values were significantly higher in the infarcted area compared with the contralateral mirror area, and significantly increased from

hyperacute to chronic phase (all P -values < 0.05) (**Table 2**).

MD, D_{\perp} decreased gradually with the time to the bottom in acute phase ($0.449 \pm 0.080 \times 10^{-3} \text{ mm}^2/\text{s}$, $0.364 \pm 0.084 \times 10^{-3} \text{ mm}^2/\text{s}$), and then started to increase gradually; D_{\parallel} decreased to the bottom in subacute phase ($0.611 \pm 0.137 \times 10^{-3} \text{ mm}^2/\text{s}$), then gradually increased (**Figure 3**). MD, D_{\parallel} , D_{\perp} value decreased in the bottom by -51.13%, -55.43%, -46.48%, respectively. MD, D_{\parallel} and D_{\perp} value in the infarcted area are significant lower than that in the contralateral mirror side in every phase (all P values < 0.05) (**Table 2**).

FA value in the infarcted area decreased from hyperacute phase to chronic phase (**Figure 3**). For FA, there was no significant difference between infarcted area and contralateral mirror area in hyperacute phase ($P = 0.315$); from acute phase to chronic phase, FA in the infarcted area were significant lower than those in the contralateral mirror side (all P values < 0.05) (**Table 2**).

Changes in the corticospinal tract of the DKI-derived variables

In the four selected area of corticospinal tract (posterior limb of internal capsule, cerebral peduncle, pons, medulla), for MK only the ipsilateral PLIC in acute and subacute phase had significant changes compared to relevant con-

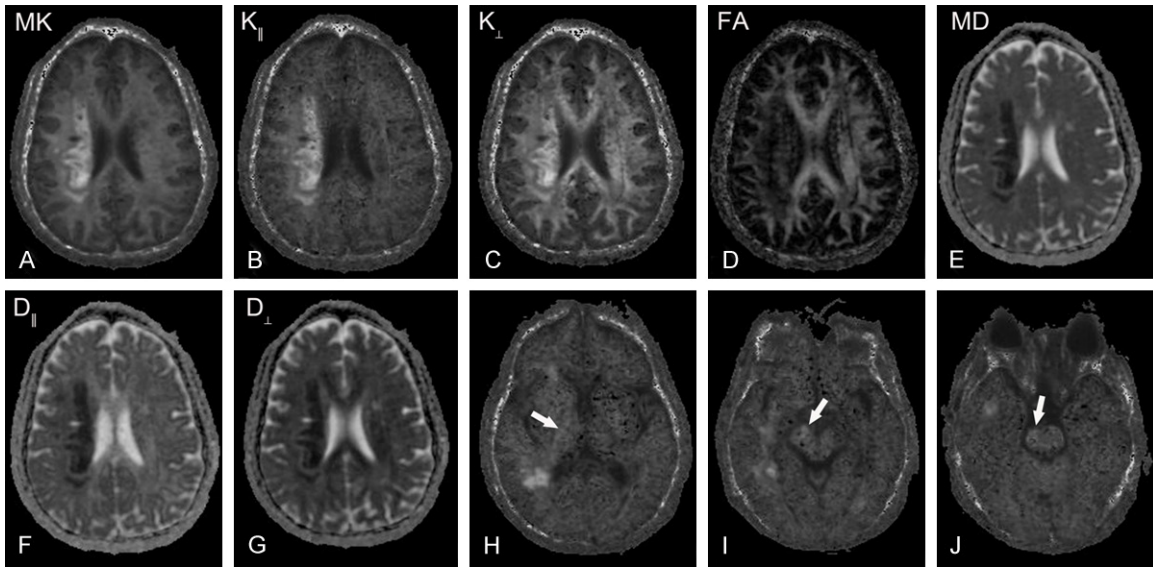


Figure 2. A 48-year-old female patient with left limb weakness for 10 days. A-G: Represent the infarcted area in MK, $K_{||}$, K_{\perp} , FA, MD, $D_{||}$, D_{\perp} map, respectively; H-J: Indicate $K_{||}$ maps in the plane of posterior limb of internal capsule (PLIC), cerebral peduncle (CP) and pons. The infarcted area in MK, $K_{||}$, K_{\perp} map showed inhomogeneous hyperintensity signal, while MD, $D_{||}$, D_{\perp} map showed relative homogeneous low signal. FA map exhibited a slightly low signal with the boundary ambiguously. The right side along corticospinal tract in the plane of PLIC, CP, and pons manifested as slightly high signal (arrow).

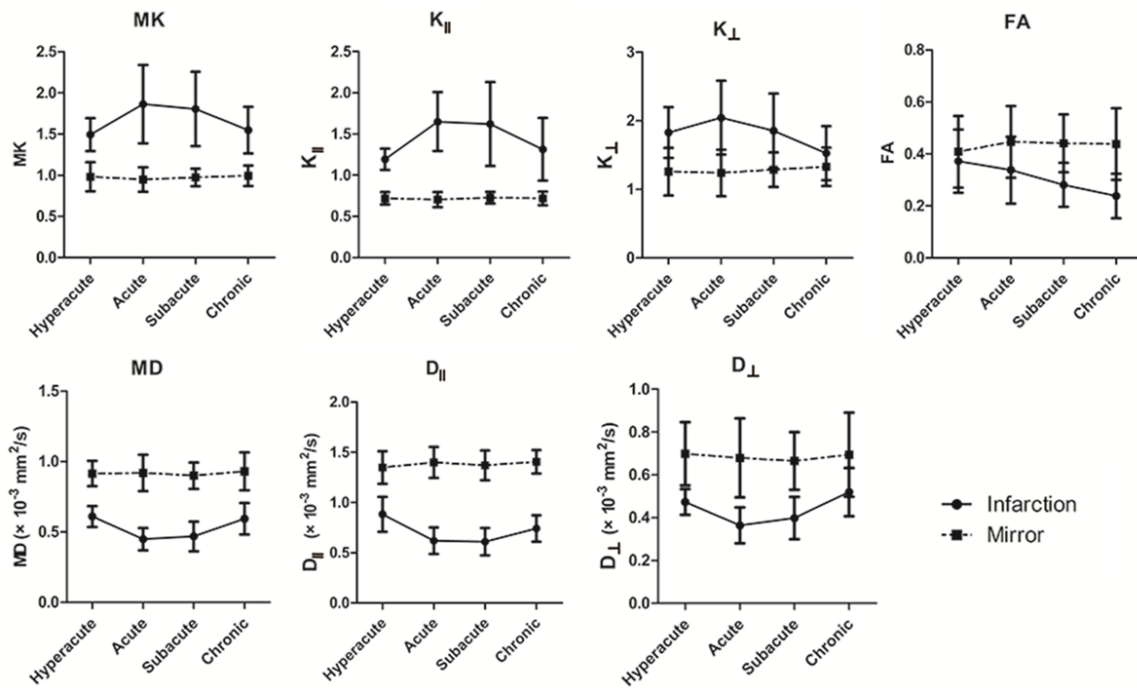


Figure 3. The evolutions of MK, $K_{||}$, K_{\perp} , FA, MD, $D_{||}$, D_{\perp} in the infarcted areas and the contralateral mirror areas MK, $K_{||}$, K_{\perp} , FA were dimensionless, MD, $D_{||}$, D_{\perp} were given in $\times 10^{-3}$ mm²/s.

tralateral areas. For $K_{||}$, PLIC and CP in acute and subacute phase, PLIC, CP and pons in chronic phase had significant changes. For K_{\perp}

in every phase, there was no significant change between two sides in the selected four planes (Table 3).

DKI in evaluating CST after infarction

Table 2. Comparison of DKI-derived variables between infarcted area and contralateral mirror area

		Hyperacute phase		Acute phase		Subacute phase		Chronic phase	
		Mean ± SD	P	Mean ± SD	P	Mean ± SD	P	Mean ± SD	P
MK	Lesion	1.495 ± 0.199	0.000*	1.864 ± 0.475	0.000*	1.806 ± 0.451	0.000*	1.548 ± 0.282	0.000*
	Mirror	0.982 ± 0.178		0.949 ± 0.148		0.974 ± 0.107		0.994 ± 0.123	
K	Lesion	1.193 ± 0.130	0.000*	1.650 ± 0.357	0.000*	1.622 ± 0.509	0.000*	1.314 ± 0.380	0.000*
	Mirror	0.718 ± 0.076		0.704 ± 0.092		0.725 ± 0.071		0.718 ± 0.081	
K _⊥	Lesion	1.828 ± 0.370	0.000*	2.045 ± 0.540	0.000*	1.853 ± 0.546	0.000*	1.528 ± 0.394	0.135
	Mirror	1.259 ± 0.348		1.238 ± 0.339		1.287 ± 0.252		1.330 ± 0.278	
MD	Lesion	0.610 ± 0.074	0.000*	0.449 ± 0.080	0.000*	0.469 ± 0.106	0.000*	0.594 ± 0.113	0.000*
	Mirror	0.915 ± 0.089		0.919 ± 0.129		0.900 ± 0.094		0.931 ± 0.134	
D	Lesion	0.883 ± 0.174	0.000*	0.621 ± 0.132	0.000*	0.611 ± 0.137	0.000*	0.743 ± 0.131	0.000*
	Mirror	1.349 ± 0.161		1.400 ± 0.154		1.371 ± 0.148		1.406 ± 0.117	
D _⊥	Lesion	0.473 ± 0.060	0.001*	0.364 ± 0.084	0.000*	0.398 ± 0.099	0.000*	0.519 ± 0.112	0.001*
	Mirror	0.698 ± 0.148		0.679 ± 0.185		0.665 ± 0.135		0.694 ± 0.197	
FA	Lesion	0.372 ± 0.122	0.315	0.338 ± 0.129	0.000*	0.281 ± 0.085	0.000*	0.238 ± 0.086	0.000*
	Mirror	0.408 ± 0.138		0.447 ± 0.138		0.441 ± 0.111		0.438 ± 0.138	

MK: mean kurtosis, K_{||}: axial kurtosis, K_⊥: radial kurtosis, FA: fractional anisotropy, MD: mean diffusion coefficient, D_{||}: axial diffusion coefficient, D_⊥: radial diffusion coefficient. Lesion and Mirror means the infarcted area and the contralateral mirror area, respectively. *denotes significant difference between infarcted area and the contralateral mirror area. MK, K_{||}, K_⊥, FA were dimensionless, MD, D_{||}, D_⊥ were given in × 10⁻³ mm²/s.

Table 3. Comparison of DKI metrics (MK, K_{||}, K_⊥) between two sides of corticospinal tract

		Hyperacute phase		Acute phase		Subacute phase		Chronic phase	
		Mean ± SD	P	Mean ± SD	P	Mean ± SD	P	Mean ± SD	P
MK_PLIC	Ipsi	1.164 ± 0.055	0.833	1.204 ± 0.167	0.035*	1.271 ± 0.239	0.009*	1.188 ± 0.133	0.069
	Contra	1.169 ± 0.074		1.133 ± 0.066		1.161 ± 0.097		1.137 ± 0.089	
MK_CP	Ipsi	1.005 ± 0.140	0.751	0.991 ± 0.073	0.608	0.990 ± 0.111	0.195	0.994 ± 0.080	0.673
	Contra	1.014 ± 0.171		0.998 ± 0.087		0.974 ± 0.099		0.988 ± 0.057	
MK_Pons	Ipsi	1.043 ± 0.049	0.075	1.052 ± 0.067	0.910	1.040 ± 0.053	0.872	1.051 ± 0.071	0.256
	Contra	1.063 ± 0.053		1.051 ± 0.099		1.042 ± 0.061		1.036 ± 0.083	
MK_Medulla	Ipsi	0.922 ± 0.067	0.331	0.875 ± 0.060	0.583	0.874 ± 0.069	0.284	0.888 ± 0.049	0.681
	Contra	0.909 ± 0.060		0.880 ± 0.052		0.955 ± 0.406		0.892 ± 0.036	
K _PLIC	Ipsi	0.631 ± 0.026	0.679	0.697 ± 0.134	0.045*	0.765 ± 0.205	0.000*	0.755 ± 0.170	0.006*
	Contra	0.624 ± 0.056		0.632 ± 0.070		0.607 ± 0.038		0.611 ± 0.063	
K _CP	Ipsi	0.639 ± 0.058	0.401	0.658 ± 0.042	0.046*	0.676 ± 0.100	0.001*	0.708 ± 0.080	0.008*
	Contra	0.654 ± 0.066		0.631 ± 0.055		0.643 ± 0.096		0.652 ± 0.067	
K _Pons	Ipsi	0.835 ± 0.075	0.741	0.790 ± 0.063	0.996	0.790 ± 0.065	0.972	0.799 ± 0.051	0.008*
	Contra	0.830 ± 0.054		0.790 ± 0.088		0.791 ± 0.059		0.763 ± 0.057	
K _Medulla	Ipsi	0.811 ± 0.080	0.298	0.805 ± 0.056	0.095	0.773 ± 0.061	0.413	0.779 ± 0.057	0.763
	Contra	0.797 ± 0.057		0.786 ± 0.060		0.782 ± 0.062		0.785 ± 0.048	
K _⊥ _PLIC	Ipsi	1.810 ± 0.190	0.442	1.892 ± 0.367	0.051	1.937 ± 0.332	0.393	1.679 ± 0.289	0.135
	Contra	1.872 ± 0.182		1.745 ± 0.321		1.880 ± 0.267		1.764 ± 0.276	
K _⊥ _CP	Ipsi	1.406 ± 0.266	0.786	1.346 ± 0.228	0.132	1.339 ± 0.175	0.820	1.328 ± 0.215	0.210
	Contra	1.389 ± 0.278		1.407 ± 0.240		1.346 ± 0.202		1.375 ± 0.219	
K _⊥ _Pons	Ipsi	1.510 ± 0.135	0.104	1.496 ± 0.269	0.986	1.459 ± 0.166	0.623	1.486 ± 0.251	0.795
	Contra	1.559 ± 0.101		1.497 ± 0.259		1.475 ± 0.147		1.474 ± 0.193	
K _⊥ _Medulla	Ipsi	1.149 ± 0.153	0.566	1.073 ± 0.168	0.852	1.083 ± 0.167	0.657	1.144 ± 0.138	0.698
	Contra	1.175 ± 0.119		1.078 ± 0.183		1.066 ± 0.151		1.131 ± 0.109	

MK: mean kurtosis, K_{||}: axial kurtosis, K_⊥: radial kurtosis; PLIC: posterior limb of internal capsule, CP: cerebral peduncle; Ipsi and contra represented ipsilateral and contralateral side with the infarcted area; *denotes significant difference between two sides; MK, K_{||}, K_⊥ were dimensionless.

DKI in evaluating CST after infarction

Table 4. Comparison of DTI metrics (MD, D_{\parallel} , D_{\perp} , FA) between two sides of corticospinal tract

		Hyperacute phase		Acute phase		Subacute phase		Chronic phase	
		Mean \pm SD	P						
MD_PLIC	Ipsi	0.833 \pm 0.058	0.489	0.813 \pm 0.101	0.038*	0.794 \pm 0.105	0.009*	0.827 \pm 0.110	0.041*
	Contra	0.841 \pm 0.055		0.857 \pm 0.075		0.847 \pm 0.037		0.871 \pm 0.098	
MD_CP	Ipsi	0.941 \pm 0.074	0.784	0.941 \pm 0.056	0.234	0.916 \pm 0.080	0.001*	0.938 \pm 0.122	0.575
	Contra	0.934 \pm 0.125		0.959 \pm 0.085		0.955 \pm 0.074		0.947 \pm 0.076	
MD_Pons	Ipsi	0.816 \pm 0.039	0.109	0.839 \pm 0.070	0.470	0.833 \pm 0.046	0.606	0.859 \pm 0.104	0.097
	Contra	0.803 \pm 0.041		0.851 \pm 0.106		0.837 \pm 0.061		0.881 \pm 0.143	
MD_Medulla	Ipsi	0.954 \pm 0.133	0.341	0.895 \pm 0.058	0.401	0.958 \pm 0.114	0.750	0.956 \pm 0.129	0.406
	Contra	0.937 \pm 0.123		0.902 \pm 0.058		0.954 \pm 0.094		0.947 \pm 0.120	
D_{\parallel} _PLIC	Ipsi	1.502 \pm 0.127	0.046*	1.515 \pm 0.189	0.049*	1.438 \pm 0.245	0.000*	1.433 \pm 0.258	0.021*
	Contra	1.574 \pm 0.092		1.617 \pm 0.142		1.655 \pm 0.086		1.609 \pm 0.073	
D_{\parallel} _CP	Ipsi	1.652 \pm 0.093	0.590	1.638 \pm 0.079	0.115	1.570 \pm 0.171	0.000*	1.523 \pm 0.171	0.034*
	Contra	1.621 \pm 0.163		1.683 \pm 0.135		1.649 \pm 0.140		1.611 \pm 0.092	
D_{\parallel} _Pons	Ipsi	1.259 \pm 0.067	0.433	1.340 \pm 0.079	0.436	1.294 \pm 0.072	0.099	1.319 \pm 0.096	0.013*
	Contra	1.245 \pm 0.079		1.354 \pm 0.121		1.319 \pm 0.093		1.370 \pm 0.131	
D_{\parallel} _Medulla	Ipsi	1.317 \pm 0.149	0.599	1.291 \pm 0.074	0.503	1.362 \pm 0.120	0.998	1.345 \pm 0.141	0.757
	Contra	1.330 \pm 0.133		1.300 \pm 0.083		1.362 \pm 0.112		1.354 \pm 0.129	
D_{\perp} _PLIC	Ipsi	0.499 \pm 0.087	0.157	0.462 \pm 0.093	0.504	0.471 \pm 0.077	0.065	0.525 \pm 0.115	0.194
	Contra	0.474 \pm 0.065		0.478 \pm 0.113		0.443 \pm 0.040		0.502 \pm 0.146	
D_{\perp} _CP	Ipsi	0.586 \pm 0.095	0.831	0.593 \pm 0.077	0.820	0.590 \pm 0.065	0.102	0.645 \pm 0.155	0.078
	Contra	0.590 \pm 0.122		0.597 \pm 0.099		0.608 \pm 0.068		0.615 \pm 0.110	
D_{\perp} _Pons	Ipsi	0.595 \pm 0.042	0.137	0.588 \pm 0.079	0.589	0.602 \pm 0.049	0.569	0.629 \pm 0.122	0.624
	Contra	0.583 \pm 0.034		0.599 \pm 0.118		0.596 \pm 0.062		0.636 \pm 0.159	
D_{\perp} _Medulla	Ipsi	0.773 \pm 0.127	0.070	0.697 \pm 0.068	0.625	0.756 \pm 0.124	0.739	0.761 \pm 0.138	0.149
	Contra	0.740 \pm 0.124		0.703 \pm 0.062		0.750 \pm 0.109		0.743 \pm 0.126	
FA_PLIC	Ipsi	0.604 \pm 0.087	0.077	0.639 \pm 0.071	0.513	0.604 \pm 0.087	0.000*	0.558 \pm 0.126	0.023*
	Contra	0.639 \pm 0.057		0.654 \pm 0.099		0.683 \pm 0.036		0.635 \pm 0.099	
FA_CP	Ipsi	0.574 \pm 0.072	0.522	0.566 \pm 0.058	0.451	0.548 \pm 0.054	0.272	0.499 \pm 0.103	0.021*
	Contra	0.564 \pm 0.072		0.577 \pm 0.067		0.558 \pm 0.048		0.542 \pm 0.077	
FA_Pons	Ipsi	0.478 \pm 0.038	0.585	0.510 \pm 0.047	0.617	0.485 \pm 0.036	0.081	0.470 \pm 0.072	0.228
	Contra	0.482 \pm 0.035		0.504 \pm 0.061		0.498 \pm 0.044		0.483 \pm 0.074	
FA_Medulla	Ipsi	0.332 \pm 0.031	0.001*	0.371 \pm 0.049	0.922	0.363 \pm 0.057	0.952	0.353 \pm 0.064	0.438
	Contra	0.366 \pm 0.039		0.370 \pm 0.039		0.363 \pm 0.064		0.364 \pm 0.053	

MD: mean diffusion coefficient, D_{\parallel} : axial diffusion coefficient, D_{\perp} : radial diffusion coefficient, FA: fractional anisotropy. PLIC: posterior limb of internal capsule, CP: cerebral peduncle; *denotes significant difference between two sides. MD, D_{\parallel} , D_{\perp} were given in $\times 10^{-3}$ mm²/s, FA was dimensionless.

For MD, PLIC in acute phase, PLIC and CP in subacute phase, PLIC in chronic phase had significant changes. For D_{\parallel} , PLIC in hyperacute and acute phase, PLIC and CP in subacute phase, PLIC, CP and pons in chronic phase had significant changes. For D_{\perp} in every phase, no significant changes were seen in all the selected four planes. For FA, only medulla in hyperacute phase, PLIC in subacute phase, PLIC and CP in chronic phase showed significant changes (Table 4).

MK, K_{\parallel} , K_{\perp} value in the ipsilateral areas that have significant changes were higher than that

in the contralateral areas, and MD, D_{\parallel} , D_{\perp} , FA value in the ipsilateral areas that have significant changes were lower than that in the contralateral areas.

Comparison of DKI and DTI metrics in evaluating the changes of CST

In all of the above variables, K_{\parallel} and D_{\parallel} were more helpful to detect the subtle change of CST after unilateral cerebral infarction; they both had seven locations that had significant changes in all phases. Moreover, there were more locations that had significant changes with the

time going on. For MK, MD and FA, there were just two to four locations in all phases that had significant changes. And for K_{\perp} , D_{\perp} , no significant change was seen in all the locations and in all phases.

Discussion

This study demonstrated the feasibility of DKI in evaluating the ischemic lesion and the microstructure change of the descending CST, which may reflect the extent of Wallerian degeneration after unilateral cerebral infarction solely in middle cerebral artery territory. The DKI derived variables in the ischemic lesion all have the peak value in acute phase. K_{\parallel} and D_{\parallel} are more helpful to detect the subtle change of CST in all the DKI derived variables.

MK, K_{\parallel} , K_{\perp} value in the infarcted area increased to the peak in acute phase, then gradually decreased; MD, D_{\parallel} and D_{\perp} value decreased to the bottom in acute phase then they started to increase gradually (**Figure 3**); they also had the biggest percent change in acute phase. From this, it can be predicted that the infarcted area may have severe pathophysiological change in acute phase; this also play an important role in the high signal manifested on MK maps. Previous DKI studies of stroke [13-17] have shown that the high signal on MK maps indicate an increase in the complexity or heterogeneity of the cellular microenvironment. So DKI can provide more detailed diffusion information in patients with ischemic stroke. The continuous decrease of FA over time represented a persistent destruction in the infarcted area, mainly the loss of myelin and the restricted water molecular movement due to the loss of ordered structures. It was a chronic process lasting a minimum time period of 3-6 months [18].

In this DKI study, the abnormal area of ipsilateral corticospinal tract manifested as hyperintensity on MK, K_{\parallel} , K_{\perp} maps (**Figure 2**), while on MD, D_{\parallel} , D_{\perp} and FA maps they were hypointensity. Wen et al [5] reported that Wallerian degeneration can be detected as early as the second day after modeling by diffusion tensor imaging in a cat Wallerian degeneration model. In our study, on D_{\parallel} maps, ipsilateral corticospinal tract can be detected with significant change in the plane of PLIC early in hyperacute phase. With the time going on, more locations

can be detected with significant changes. The different diffusion variables also showed different sensitivity to evaluate the microstructure change of CST. One thing should be noted that, the time to detect the degenerated CST varied with species and the Wallerian degeneration models, and other circumstances. We also see that there was almost no significant difference between two sides of CST in the plane of medulla. This is probably mainly due to some fibers of the descending CST cross to the other side on this plane, the difference between two sides can't be observed.

Fan's study [2] showed that ADC increased in the affected side of CST in a rat Wallerian degeneration model, while Xiang's research [4] found that ADC significantly decreased in 8 patients 3 to 21 days after stroke onset. In our study, MD, which has the analogous meaning as ADC, in the ipsilateral areas that have significant changes are lower than that in the contralateral areas. Thus, different results generated. Wen et al [5] dynamically observed the diffusion indices of DTI in a cat Wallerian degeneration model, and found that, during the early stage (within 8 days after modeling), MD in the affected side showed instability, while in the late stage (after 8 days), MD gradually increased. It can be speculated that, MD experienced a process from decrease to normalization, then increase in the affected side of CST.

Based on the above results, K_{\parallel} and D_{\parallel} are more helpful to detect the subtle change of CST after unilateral cerebral infarction. The pathological change of corticospinal tract after infarction was mainly due to the damage of axons; and it may be severe than the proximal myelin sheaths injury. This can explain why the extent of Wallerian degeneration of CST correlates well with the clinical motor deficit [1, 19]. So K_{\parallel} , D_{\parallel} may be a new biomarker to reflect the injury extent of CST Wallerian degeneration, this can reflect patient's prognosis and may be helpful in making clinical decision.

As for MK, MD and FA, fewer locations that have significant changes were detected in all phases. The subjects enrolled in this study were in a relative early phase of infarction, more locations can be detected if the ischemic patients were in a stage of 3-6 months, or longer. Several diffusion tensor imaging (DTI) studies [4, 7, 19, 20] also demonstrated FA value

decreased significantly, and correlates well with the motor deficit.

One limitation of this study is that the included subjects had no clinical data of motor deficit, so the correlation of DKI-derived variables and the limb motor deficit couldn't be calculated. More detailed studies should be done to in-depth understand the application of DKI in evaluating Wallerian degeneration.

In conclusion, DKI can provide more detailed diffusion information in patients with ischemic stroke. Among all the DKI-derived variables, K_{\parallel} and D_{\parallel} are more helpful to early detect the micro pathological changes of the descending CST after unilateral cerebral infarction. The pathological change of Wallerian degeneration is probably mainly due to the obstruction of axons. So DKI, especially the variable K_{\parallel} and D_{\parallel} , may serve as a new biomarker to early observe the minor change of the descending CST, which can reflect patient's prognosis and give a good help for clinical decision making.

Acknowledgements

This work was supported by grants from the National Program of the Ministry of Science and Technology of China during the "12th Five-Year Plan" (No. 2011BAI08B10), Major State Basic Research Development Program of China (973 Program) (No. 2013CB733803) and National Natural Science Foundation of China (No. 81171308, 81570462). The authors thank Ping Yin and Wenhua Liu, for their advice and assistance in the statistical analysis.

Disclosure of conflict of interest

None.

Address correspondence to: Dr. Wenzhen Zhu, Department of Radiology, Tongji Hospital, Tongji Medical College, Huazhong University of Science and Technology, Wuhan 430030, China. Tel: +86-27-83663258; E-mail: zhuwenzhen8612@163.com; Dr. Cong-Yi Wang, The Center for Biomedical Research, Key Laboratory of Organ Transplantation, Ministry of Health & Ministry of Education, Tongji Hospital, Tongji Medical College, Huazhong University of Science and Technology, 1095 Jiefang Ave., Wuhan 430030, China. Tel: +86-27-83663485; E-mail: wangcy@tjh.tjmu.edu.cn

References

- [1] DeVetten G, Coutts SB, Hill MD, Goyal M, Eesa M, O'Brien B, Demchuk AM, Kirton A; MONITOR and VISION study groups. Acute corticospinal tract wallerian degeneration is associated with stroke outcome. *Stroke* 2010; 41: 751-756.
- [2] Zhang F, Lu GM and Zee CS. Comparative study of the sensitivity of ADC value and T(2) relaxation time for early detection of Wallerian degeneration. *Eur J Radiol* 2011; 79: 118-123.
- [3] Domi T, deVeber G, Shroff M, Kouzmitcheva E, MacGregor DL and Kirton A. Corticospinal tract pre-wallerian degeneration: a novel outcome predictor for pediatric stroke on acute MRI. *Stroke* 2009; 40: 780-787.
- [4] Liu X, Tian W, Li L, Kolar B, Qiu X, Chen F and Dogra VS. Hyperintensity on diffusion weighted image along ipsilateral cortical spinal tract after cerebral ischemic stroke: a diffusion tensor analysis. *Eur J Radiol* 2012; 81: 292-297.
- [5] Qin W, Zhang M, Piao Y, Guo D, Zhu Z, Tian X, Li K and Yu C. Wallerian degeneration in central nervous system: dynamic associations between diffusion indices and their underlying pathology. *PLoS One* 2012; 7: e41441.
- [6] Grassel D, Ringer TM, Fitzek C, Fitzek S, Kohl M, Kaiser WA, Witte OW and Axer H. Wallerian degeneration of pyramidal tract after paramedian pons infarct. *Cerebrovasc Dis* 2010; 30: 380-388.
- [7] Shen Y, Li M, Wei R and Lou M. Effect of acupuncture therapy for postponing Wallerian degeneration of cerebral infarction as shown by diffusion tensor imaging. *J Altern Complement Med* 2012; 18: 1154-1160.
- [8] Fieremans E, Jensen JH and Helpert JA. White matter characterization with diffusional kurtosis imaging. *Neuroimage* 2011; 58: 177-188.
- [9] Jensen JH and Helpert JA. MRI quantification of non-gaussian water diffusion by kurtosis analysis. *NMR Biomed* 2010; 23: 698-710.
- [10] Wu EX and Cheung MM. MR diffusion kurtosis imaging for neural tissue characterization. *NMR Biomed* 2010; 23: 836-848.
- [11] Steven AJ, Zhuo J and Melhem ER. Diffusion kurtosis imaging: an emerging technique for evaluating the microstructural environment of the brain. *AJR Am J Roentgenol* 2014; 202: W26-33.
- [12] Tabesh A, Jensen JH, Ardekani BA and Helpert JA. Estimation of tensors and tensor-derived measures in diffusional kurtosis imaging. *Magn Reson Med* 2011; 65: 823-836.
- [13] Taoka T, Fujioka M, Sakamoto M, Miyasaka T, Akashi T, Ochi T, Hori S, Uchikoshi M, Xu J and Kichikawa K. Time course of axial and radial

DKI in evaluating CST after infarction

- diffusion kurtosis of white matter infarctions: period of pseudonormalization. *AJNR Am J Neuroradiol* 2014; 35: 1509-1514.
- [14] Hui ES, Du F, Huang S, Shen Q and Duong TQ. Spatiotemporal dynamics of diffusional kurtosis, mean diffusivity and perfusion changes in experimental stroke. *Brain Res* 2012; 1451: 100-109.
- [15] Hui ES, Fieremans E, Jensen JH, Tabesh A, Feng W, Bonilha L, Spampinato MV, Adams R and Helpert JA. Stroke assessment with diffusional kurtosis imaging. *Stroke* 2012; 43: 2968-2973.
- [16] Cheung JS, Wang E, Lo EH and Sun PZ. Stratification of heterogeneous diffusion MRI ischemic lesion with kurtosis imaging: evaluation of mean diffusion and kurtosis MRI mismatch in an animal model of transient focal ischemia. *Stroke* 2012; 43: 2252-2254.
- [17] Jensen JH, Falangola MF, Hu C, Tabesh A, Rapalino O, Lo C and Helpert JA. Preliminary observations of increased diffusional kurtosis in human brain following recent cerebral infarction. *NMR Biomed* 2011; 24: 452-457.
- [18] Axer H, Grassel D, Bramer D, Fitzek S, Kaiser WA, Witte OW and Fitzek C. Time course of diffusion imaging in acute brainstem infarcts. *J Magn Reson Imaging* 2007; 26: 905-912.
- [19] Puig J, Pedraza S, Blasco G, Daunis IEJ, Prats A, Prados F, Boada I, Castellanos M, Sanchez-Gonzalez J, Remollo S, Laguillo G, Quiles AM, Gomez E and Serena J. Wallerian degeneration in the corticospinal tract evaluated by diffusion tensor imaging correlates with motor deficit 30 days after middle cerebral artery ischemic stroke. *AJNR Am J Neuroradiol* 2010; 31: 1324-1330.
- [20] Liu X, Tian W, Qiu X, Li J, Thomson S, Li L and Wang HZ. Correlation analysis of quantitative diffusion parameters in ipsilateral cerebral peduncle during wallerian degeneration with motor function outcome after cerebral ischemic stroke. *J Neuroimaging* 2012; 22: 255-260.